Energy Spectrum of the Soft Component near Sea Level

HUGH CARMICHAEL
Chalk River Laboratories, Atomic Energy of Canada Limited, Chalk River, Ontario, Canada
(Received May 17, 1957)

An analysis of the transition curves of Carmichael and Steljes has been carried out to yield the transition curves in lead of ion-chamber bursts produced by cascades initiated by the electrons and photons of the soft component incident from the atmosphere. From the rates at the maxima of these transition curves, the absolute omnidirectional integral energy spectrum of the electrons and photons of the soft component at sea level, in the energy range from about 100 Mev to 100 Bev, is deduced. Incident electrons and photons associated with extensive air showers, as identified by coincidences with a nearby larger ion chamber, are excluded. An additional single experimental point on the integral spectrum (8.4×10^{-3} per sphere of unit area per sec) is obtained from the observed rate of electrons of all energies greater than 1 Mev which intersect the unshielded ion chamber. Since a quantitative relation from electromagnetic cascade theory is made use of in the derivation of the energy spectrum, and since this relation is at present uncertain for lead in the energy range involved, the possible error of the flux in the energy spectrum ($\pm100\%$) is much larger than that of the observed rates of occurrence of bursts ($\pm5\%$). In this respect the spectrum is preliminary only. In the energy range below 400 Mev the integral spectrum is in agreement with previous absolute measurements; below 2 Bev it is in conformity with a previous relative measurement; from 1.6 Bev to 100 Bev, where there are no previous determinations, it obeys a power law of exponent -2.00 and the rate for 1.6 Bev is 2.4×10^{-5} per sphere of unit area per sec.

1. INTRODUCTION

THE ionization bursts produced by the omnidirectional flux of cosmic radiation, near sea level, in a spherical, 8-inch diameter, pressurized ion chamber, unshielded and with 15 different thicknesses of hemispherical lead shielding, have been reported in I and II.[1] It was shown that the bursts arising from μ mesons and protons intersecting the ion chamber, from stars in the gas, and from extensive air showers could be determined for each thickness of the lead shield and subtracted.

In the unshielded ion chamber the bursts that remained after subtraction were ascribed to the electrons of the soft component that were not associated with detected extensive air showers. These electrons are more than 100 times as numerous as the detected extensive showers (see Fig. 4 of I). No doubt some of them come from the fringes of undetected air showers but the majority are probably connected with primary showers only indirectly, for example through knock-on and decay processes of μ mesons in which electrons may occur at a great distance from the primary shower. From the shape of their pulse-size distribution, and its similarity to the shape of the distribution produced by the μ mesons which are known to occur singly, it is inferred that, within the area (324 cm^2) presented by the ion chamber, nearly all of these electrons of the soft component occur singly.

Under the lead shields the bursts that remained after subtraction were ascribed to, (a) electromagnetic cascades arising from electrons and photons incident on the shield from the atmosphere, (b) electromagnetic cascades originating within the lead from knock-on and radiation by μ mesons, and (c) penetrating showers and electromagnetic cascades engendered within the lead from the nucleonic component. The results were presented as a family of transition curves in lead for bursts of different given sizes measured in ion-pairs. One of the transition curves (for bursts of exactly 4.27×10^6 ion-pairs or an average of 32 particles) is shown in Fig. 1 where a broken line indicates a separation between bursts of type (a), arising from electrons and photons incident on the shield, and bursts of types (b) and (c), engendered within the lead.

One objective of the present paper is to separate the bursts of type (a) from those of types (b) and (c) and so obtain the transition curves in lead arising from the incident electrons and photons not associated with detected air showers. These transition curves represent mainly the propagation of single cascades in lead and so they are suitable for comparison with calculations of the electromagnetic cascade process. At the same time the energy spectrum of the incident electrons and photons of the soft component can be derived from the measured rates of cascades of different size. In fact each individual transition curve contains bursts originating from incident electrons or photons in a range of energies and so calculation of the shape of even a single transition curve requires both a correct electromagnetic cascade theory and a knowledge of the energy spectrum of the incident particles over the appropriate range of energy. Also, for a valid calculation, the effect of the spherical geometry of the ion chamber and of the shielding must be allowed for in detail.

It has not so far been possible to make a satisfactory comparison between theory and experiment because of the lack of tabulated results of cascade-theory calculations applicable specifically to lead in the range of energies up to 100 Bev. It is well known that conventional cascade theory is only valid for elements of low atomic number. A Monte Carlo calculation of cascades in lead in the energy range below 500 Mev, made by Wilson,[2] showed that the number of electrons emerging from a lead plate in the vicinity of the cascade maximum

[1] H. Carmichael and J. F. Steljes, Phys. Rev. **99**, 1542 (1955); **105**, 1626 (1957). These papers will be referred to as I and II, respectively.

[2] R. R. Wilson, Phys. Rev. **86**, 261 (1952).

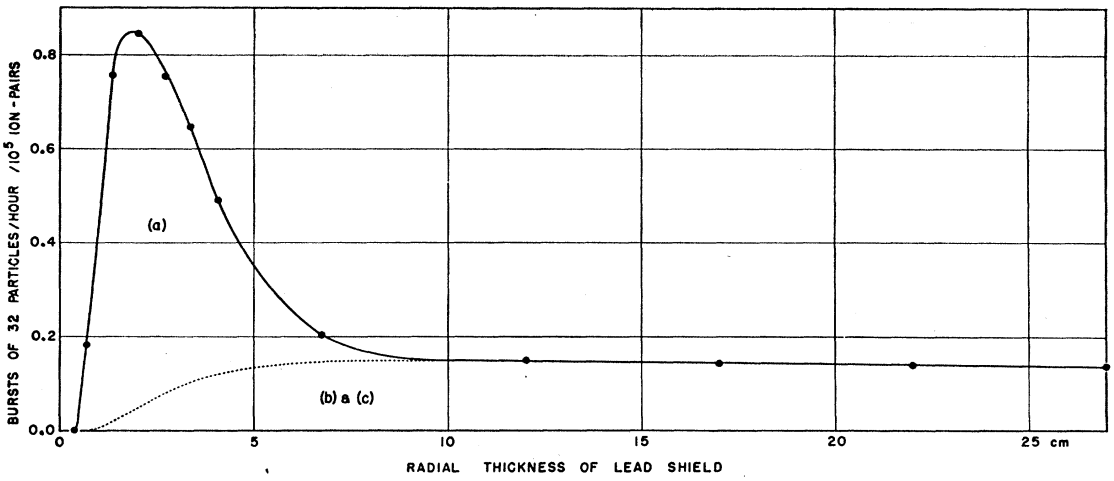

FIG. 1. The transition curve for bursts of 4.27×10^6 ion-pairs, or an average of 32 particles crossing the ion chamber. The broken line indicates a separation between, (a), bursts arising from cascades produced by electrons or photons incident on the shield from the atmosphere and, (b) and (c), bursts arising from cascades initiated by μ mesons or in penetrating showers.

is less than that given by conventional theory by a factor of about 2. Wilson showed also that conventional theory provides cascades in lead that die away much too rapidly after the maximum. It is expected that the results of an adequate theoretical calculation for lead may become available in the near future.

A trial calculation of the transition curves was made using Wilson's data for the lower energies and the curves given by Snyder and Serber, shown in Rossi's book,[3] for the higher energies. This calculation took account of the spherical geometry of the ion chamber and the shield but did not include any allowance for the effect of statistical fluctuations of the number of particles in the cascades. The agreement of Wilson's data with the experimental transition curves was reasonably good, but the Snyder-Serber data did not give nearly a sufficient number of bursts beyond the maxima of the transition curves which is consistent with the statement that this theory yields cascades that have too few particles beyond the cascade maximum in lead. One was able to conclude, however, that it might be possible, using a correct energy spectrum and a correct theory along with proper allowance for fluctuations, to reproduce the experimental transition curves to within a few percent over the whole observed energy range from 136 Mev to 78 Bev. In other words there was no indication that the observed cascades did not originate almost entirely from single incident electrons or photons and the experimental accuracy appeared to be good. Since the discrepancies that are likely to be found between cascade-theory calculations and experiment, due for example to neglect of the trident process or to improper estimation of the fluctuations, are not expected to be large, there is no point in publishing a comparison until valid theoretical data is available.

During the course of these calculations it became clear that a useful first approximation to the energy spectrum of the soft component could be obtained from the data using from theory only the estimated number of electrons at the maximum of a cascade expressed as a function of the energy of the initiating particle.

To present this preliminary energy spectrum and compare it with previous work is the main objective of the present paper.

2. EXPERIMENTAL DATA

The experimental data to be discussed are the transition curves already extracted and published in Table III of II. In order to isolate from each of these composite transition curves the part to be ascribed to electromagnetic cascades generated by electrons or photons incident on the lead shield from the atmosphere, the true shape of the demarkation curve already mentioned, and indicated in Fig. 1, must be found. The problem of making an analytical calculation of the shape of this curve for each of the transition curves would be very difficult and the result of such a calculation for lead would at present be suspect. Fortunately, the experimental transition curve itself provides the means for an empirical solution that appears to be satisfactory.

We make the assumptions, (1) that the bursts observed under thick lead, including those arising from the nucleonic component, are produced mainly by electromagnetic cascades; i.e., that the proportion of bursts of a given measured size produced directly by the ionization of the multiple mesons and the heavier particles of the penetrating showers is negligibly small, (2) that the energy spectrum of the electrons and photons directly generated within the lead by mesons

[3] B. Rossi, *High-Energy Particles* (Prentice-Hall, Inc., New York, 1952), p. 259.

TABLE I. Differential size-frequency distributions and transition curves of bursts attributed to cascades produced by omnidirectional electrons and photons incident from the atmosphere. The figures in the body of the table are the logarithms to base ten of the omnidirectional rates per sq cm per sec per 10^5 ion-pairs.

$\log_{10}$ (size in ion-pairs)	Radial thickness of lead shield (cm)															
	0	0.110	0.262	0.360	0.67	1.35	2.02	2.70	3.36	4.04	5.39	6.73	12.0	17.0	22.0	27.0
4.8	4.14	4.20	4.15	4.10	4.01	3.82	3.66	3.48	3.29	3.10	2.85	2.39	1.58			
4.9	3.70	3.92	3.88	3.85	3.80	3.61	3.45	3.27	3.11	2.92	2.67	2.29	1.47			
5.0	3.32	3.62	3.62	3.63	3.59	3.37	3.22	3.07	2.90	2.74	2.47	2.18	1.23			
5.1	2.97	3.32	3.34	3.37	3.37	3.16	3.01	2.84	2.70	2.55	2.39	2.02	1.05			
5.2	2.44	2.97	3.04	3.11	3.13	2.96	2.78	2.63	2.47	2.32	2.09	1.77	0.82			
5.3	1.89	2.56	2.71	2.79	2.85	2.72	2.57	2.42	2.27	2.12	1.85	1.51	0.55			
5.4	0.96	2.15	2.32	2.42	2.54	2.45	2.31	2.18	2.02	1.87	1.62	1.22	0.28			
5.5		1.69	1.92	2.05	2.23	2.19	2.06	1.95	1.80	1.65	1.37	1.14	0.03			
5.6		1.24	1.49	1.64	1.90	1.96	1.81	1.70	1.56	1.39	1.13	0.77	0.59			
5.7		0.74	1.04	1.22	1.57	1.68	1.60	1.48	1.31	1.15	0.85	0.49	$\bar{1}$.41			
5.8		0.21	0.58	0.78	1.21	1.42	1.36	1.23	1.07	0.90	0.60	0.26	$\bar{1}$.16			
5.9		$\bar{1}$.65	0.11	0.33	0.87	1.13	1.10	0.99	0.81	0.65	0.31	$\bar{1}$.97	$\bar{2}$.51			
6.0		$\bar{1}$.02	$\bar{1}$.59	$\bar{1}$.86	0.48	0.84	0.81	0.72	0.57	0.37	0.05	$\bar{1}$.67	$\bar{2}$.03			
6.1			$\bar{1}$.06	$\bar{1}$.38	0.08	0.54	0.52	0.45	0.32	0.12	$\bar{1}$.75	$\bar{1}$.38	$\bar{3}$.52			
6.2				$\bar{2}$.92	$\bar{1}$.68	0.21	0.22	0.14	0.04	$\bar{1}$.84		$\bar{1}$.08				
6.3					$\bar{1}$.25	$\bar{1}$.87	$\bar{1}$.91	$\bar{1}$.83	$\bar{1}$.74	$\bar{1}$.57		$\bar{2}$.76				
6.4					$\bar{2}$.81	$\bar{1}$.51	$\bar{1}$.58	$\bar{1}$.52	$\bar{1}$.43	$\bar{1}$.27		$\bar{2}$.51				
6.5					$\bar{2}$.36	$\bar{1}$.13	$\bar{1}$.26	$\bar{1}$.21	$\bar{1}$.15	$\bar{1}$.01		$\bar{2}$.22				
6.6					$\bar{3}$.91	$\bar{2}$.73	$\bar{2}$.93	$\bar{2}$.89	$\bar{2}$.84	$\bar{2}$.72		$\bar{3}$.94				
6.7					$\bar{3}$.44	$\bar{2}$.35	$\bar{2}$.59	$\bar{2}$.61	$\bar{2}$.52	$\bar{2}$.44		$\bar{3}$.64				
6.8					$\bar{4}$.96	$\bar{3}$.94	$\bar{2}$.25	$\bar{2}$.29	$\bar{2}$.22	$\bar{2}$.14		$\bar{3}$.34				
6.9					$\bar{5}$.80	$\bar{3}$.54	$\bar{3}$.91	$\bar{3}$.99	$\bar{3}$.90	$\bar{3}$.84		$\bar{3}$.06				
7.0						$\bar{3}$.12	$\bar{3}$.56	$\bar{3}$.67	$\bar{3}$.59	$\bar{3}$.54		$\bar{4}$.80				
7.1						$\bar{4}$.70	$\bar{3}$.22	$\bar{3}$.35	$\bar{3}$.29	$\bar{3}$.25		$\bar{4}$.51				
7.2						$\bar{4}$.29	$\bar{4}$.86	$\bar{3}$.03	$\bar{4}$.98	$\bar{4}$.95		$\bar{4}$.23				
7.3						$\bar{5}$.85	$\bar{4}$.49	$\bar{4}$.71	$\bar{4}$.66	$\bar{4}$.64		$\bar{5}$.95				
7.4							$\bar{4}$.13	$\bar{4}$.40	$\bar{4}$.36	$\bar{4}$.35		$\bar{5}$.69				
7.5							$\bar{5}$.77	$\bar{4}$.07	$\bar{4}$.04	$\bar{4}$.04		$\bar{5}$.41				
7.6							$\bar{5}$.42	$\bar{5}$.74	$\bar{5}$.71	$\bar{5}$.75		$\bar{5}$.09				

or in penetrating showers is not very different from that of the electrons and photons incident on the lead shield from the atmosphere, (3) that two or more overlapping simultaneous cascades do not very often contribute to the production of a single burst.

It follows that each elementary layer of the shield can be considered to generate in the lead beneath it, for each given size of burst, a transition curve which is the same as that generated by the incident flux of electrons and photons for that size of burst.

The procedure, therefore, is to obtain first a rough approximation to the transition curve for bursts of a given size by subtracting any reasonable curve of the shape shown by the broken line in Fig. 1 from the total. The growth curve of bursts of this given size produced from electrons and photons originating within the lead is then generated by adding together contributions from successive thin layers of lead until after growth of the generated curve has ceased. The generated curve is next fitted to the observed rate at any point beyond 12 cm of lead. The allowance to be made for the relatively slow absorption of the producing radiation is readily found from the observed decrease of rate with thickness of lead beyond 12 cm. The generated curve is now subtracted from the main curve to obtain a second approximation to the desired transition curve for electrons and photons incident from outside, and the whole process is repeated to give a third and final approximation.

Before the generated curve was subtracted from the main curve an additional consideration was introduced. It is known that inside lead the electromagnetic cascades that occur are almost all generated from photons, since direct production of electrons in lead, for example by the knock-on of electrons by μ mesons, is relatively much less frequent than the production of photons. The soft component from the atmosphere on the other hand, if it is not predominantly electronic near sea level, will have at least an equal number of electrons and photons of the energies here involved capable of producing cascades in lead. Photon-induced cascades tend to develop slightly later than electron-induced cascades. To make allowance for this the generated curve was bodily displaced 0.25 cm, which is about half a radiation length, towards greater thickness of lead, before being subtracted from the main curve.

The final result of these subtractions from the rates given in Table III of II yielded the figures given in

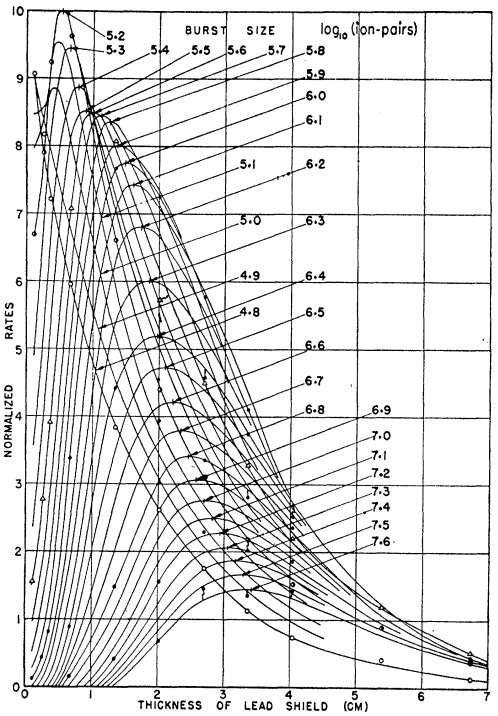

FIG. 2. The transition curves of bursts of given size produced by electromagnetic cascades incident on the lead shield from the atmosphere. The rates have been adjusted as described in the text to make the different curves comparable in size on a single graph.

Table I of this paper. There is a small discrepancy between the two tables for the largest bursts ($>10^7$ ion-pairs) in the 4.04 and 6.73 cm columns because the figures originally given in Table III of II were modified as a result of more precise fitting to the original experimental points.

In Fig. 10 of II a convenient graphical representation of transition curves for bursts of different given sizes was obtained by normalizing the rate to that observed under 27 cm of lead, where the size-frequency distribution satisfied a power law of exponent -1.73. With the same normalization factors, although the curves do not now extend beyond 12 cm of lead, the data of Table I are plotted in Fig. 2. To avoid confusion, points from Table I are shown only on each fourth curve. In drawing the curves of Fig. 2 a regular displacement of the maxima of the successive curves was imposed, in keeping with the general displacement of the experimental points. The selected position of the maximum is indicated on each curve and also given in column 2 of Table II. That it was possible to do this implies that the displacement of the maximum is a logarithmic function of the size of the bursts since the sizes are in geometrical progression.

The normalized rates of occurrence of bursts at the maximum of each of the transition curves of Fig. 2 were now read off and are given in column 3 of Table II. In column 4 the normalizing factors have been removed and the actual rates (per 10^5 ion-pair size differential) are given. In Fig. 3 these rates are shown plotted against the corresponding burst sizes. This curve is very closely related to the differential energy spectrum of the electrons and photons of the soft component. Its apparently high accuracy stems to some extent from the graphical smoothing introduced at various stages in working up the results but basically it reflects the precision of the original observations. Limits of error are discussed in Sec. 7 below.

The differential curve of Fig. 3 is a power law of exponent -3.20 for bursts of size greater than 10^6 ion-pairs. The slope changes rather suddenly near 10^6 ion-pairs to an exponent of -2.76 for all smaller bursts, except for a region of slightly enhanced rate centered around 1.6×10^5 ion-pairs. These features correspond to the variations of height of the curves of Fig. 2. The deviation around burst size 1.6×10^5 ion-pairs is in the region of bursts of average size 2 particles (in II the average[4] size of bursts due to single relativistic

TABLE II. The radial thicknesses of the lead shield and the rates, at the maxima of the transition curves, for bursts of different fixed sizes. Column 4 gives the omnidirectional rate per sq cm per sec per 10^5 ion-pairs.

$\log_{10}$ (size in ion-pairs)	Radial thickness of shield (cm Pb)	Normalized rate at transition maximum	$\log_{10}$ (actual rate at transition maximum per cm²/sec)
4.8	0.11	9.06	4.20
4.9	0.11	8.97	3.92
5.0	0.40	8.84	3.64
5.1	0.46	9.54	3.39
5.2	0.52	10.00	3.14
5.3	0.64	9.46	2.85
5.4	0.78	8.88	2.54
5.5	0.90	8.50	2.25
5.6	1.02	8.48	1.98
5.7	1.14	8.45	1.70
5.8	1.26	8.36	1.42
5.9	1.38	8.00	1.13
6.0	1.50	7.74	0.84
6.1	1.62	7.42	0.55
6.2	1.74	6.84	0.24
6.3	1.86	6.04	$\bar{1}$.92
6.4	1.98	5.18	$\bar{1}$.58
6.5	2.10	4.72	$\bar{1}$.26
6.6	2.22	4.20	$\bar{2}$.94
6.7	2.34	3.76	$\bar{2}$.62
6.8	2.46	3.38	$\bar{2}$.30
6.9	2.58	3.06	$\bar{3}$.98
7.0	2.70	2.74	$\bar{3}$.66
7.1	2.82	2.48	$\bar{3}$.34
7.2	2.94	2.27	$\bar{3}$.03
7.3	3.06	2.06	$\bar{4}$.72
7.4	3.18	1.86	$\bar{4}$.40
7.5	3.30	1.65	$\bar{4}$.07
7.6	3.42	1.44	$\bar{5}$.74

[4] This average is to be considered to apply to the whole area of the ion chamber.

particles intersecting the ion chamber was given as 6.3×10^4 ion-pairs). This suggests that this enhancement may be related to a high probability of observing electron pairs produced by the incident photons in the 50-Mev range of the spectrum.

On the basis of the average burst size produced by a single particle a figure for the average number of particles in the bursts at any point on the abscissa of Fig. 3 may be found. However, as will be seen later, this average is not a correct average for bursts produced by local cascades. From now on, therefore, we shall call it the *nominal* average number of particles in the bursts and it will be used only for labeling the transition curves in conformity with previous usage.

3. DIFFERENTIAL ENERGY SPECTRUM

The differential energy spectrum of the soft component is to be obtained by replotting the curve of Fig. 3 against the effective mean energy of the incident electrons and photons that produce the observed rate at the maximum of a transition curve instead of against the burst size in ion-pairs.

According to cascade theory, using the solution under Approximation B for electrons incident, as derived by Snyder and Serber and quoted by Rossi,[3]

$$\Pi_{\max}(E_0,0)=\frac{0.31}{[\ln(E_0/\epsilon_0)-0.37]^{\frac{1}{2}}}E_0/\epsilon_0. \qquad (1)$$

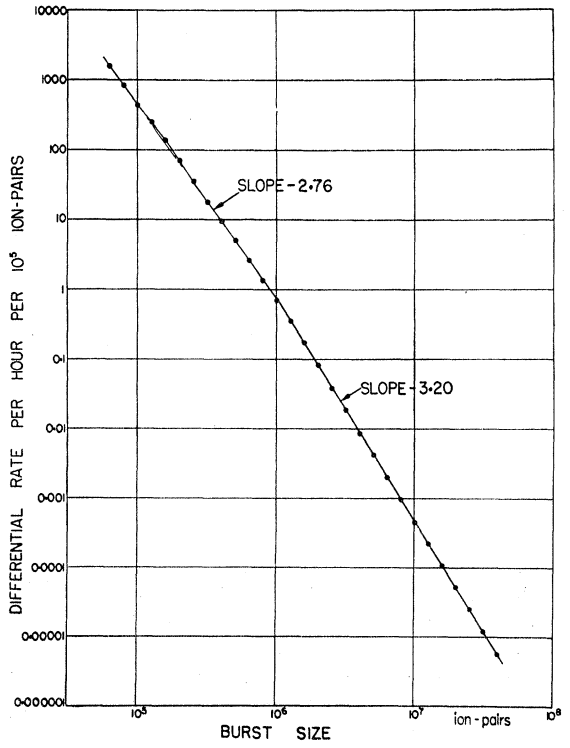

FIG. 3. The rates at the maxima of the transition curves plotted against the size of the bursts.

Here $\Pi_{\max}(E_0,0)$ is the average number of electrons at the maximum of a cascade initiated by an electron of energy E_0 in a material in which the critical energy is ϵ_0.

Since the absorber is lead and the experimental arrangement is such that there is no backscattering into the ion chamber, the number of electrons at the maximum given by (1) is too large (as discussed above) by about a factor 2. Therefore we shall use

$$2\Pi_{\max}{}^{\text{in Pb}}=\Pi_{\max}{}^{(1)}. \qquad (2)$$

For lead, $\epsilon_0=7.6$ Mev.

Since the result of cascade theory in (1) is expressed in terms of number of electrons it is necessary to express the measured size of the bursts given by the abscissa of Fig. 3 in terms of the effective average of the number of electrons in those showers that contribute to the observed rate near the maximum of a transition curve. A cascade shower emerging from the shield will tend to traverse the ion chamber in the form of a narrow pencil of electrons and so the average path length of the electrons in a particular shower will depend upon the distance of the axis of the shower from the center of the sphere. Even if there is some angular divergence of the peripheral rays of the shower, in a sphere the length of the chord along the axis of the shower will still be quite a good measure of the average path length of the electrons. Therefore, for a given size of burst, cascades passing through the middle of the ion chamber will have less than the average number of particles while cascades passing near the wall will have more than the average. Also, because of the hemispherical shape of the shield, these latter cascades will have developed in a thickness of lead considerably greater than the radial thickness of the shield. It follows that the bursts that contribute to the rate measured near the maximum of a transition curve are due, if in the central part of the ion chamber, to cascades initiated by relatively low-energy electrons or photons, or, if near the margin of the ion chamber, to cascades arising from higher energy particles. Since the incident spectrum decreases very rapidly with energy this implies that the average number of particles in bursts of a given size, at a transition-curve maximum, is weighted in favor of cascades of smaller numbers of particles.

These considerations were found to be of importance in the preliminary calculation of the transition curves referred to above—here we shall make use of a result of this calculation.[5] This result is that in the vicinity of

[5] In order to reassure the critical reader the mathematical basis may be outlined as follows. Consider single incident particles (electrons and photons) intersecting the shield along paths passing through the ion chamber at a distance r from the center. Let the energy spectrum of those particles be $S(E)dE$, and let the transition curve of bursts of a given size in ion-pairs resulting from these incident particles be $R(N,t)dN$, where N is the corresponding (fixed) number of electrons emerging from the shield into the ion chamber, t is the thickness of the shield in the line of propagation of the cascades, and $R(N,t)$ is the rate. Now E is obtainable as a function of N and t from the curves due to Snyder and Serber given in reference 3, p. 259, where N is the average number of

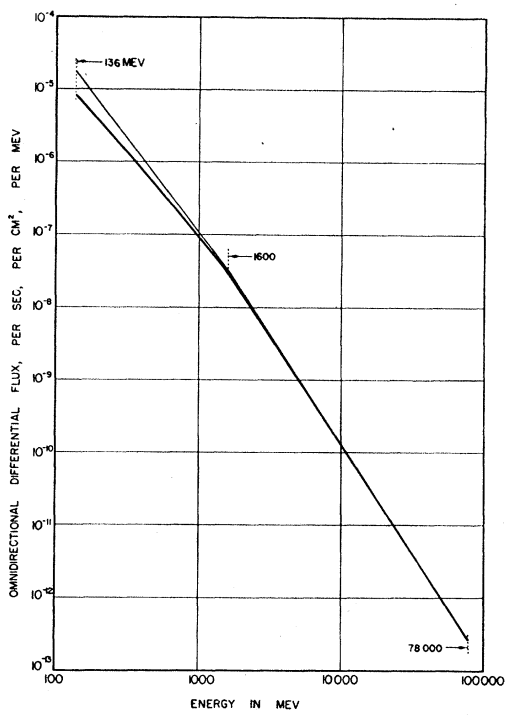

FIG. 4. The omnidirectional differential energy spectrum of the electrons and photons of the soft component. The upper curve gives the rate before making correction for the effect of statistical fluctuations of the sizes of the cascades.

the maximum of any of the transition curves the number of particles in the cascades averaged over the area of the ion chamber is only 0.83 of the nominal size obtained by division of the size in ion-pairs by the mean number of ion-pairs produced by a single particle. Therefore, after the size in ion-pairs as given on the abscissa of Fig. 3 was divided by the average number of ion-pairs produced by a single particle (6.3×10^4), it was multiplied by 0.83, to obtain the average number of particles in the cascades. Since Fig. 3 is a differential curve, when the abscissa was changed the ordinate scale was altered to conform by multiplying by the factor $(6.3\times10^4/0.83\times10^5)=0.76$ to give the rates corresponding to a size differential of one particle.

Reading from the new scales, the curve of Fig. 3 was now replotted against E_0 by means of Eqs. (1) and (2) and $\epsilon_0=7.6$ Mev. At the same time the rates were divided by the number of seconds in one hour and by the area of the ion chamber in sq cm (3600×324). The curve thus obtained is shown as the upper curve in Fig. 4 ending at 136 Mev. When this curve has been corrected for the effect of fluctuations of the number of electrons in the cascades it will represent the absolute omnidirectional differential energy spectrum of the soft component near sea level. The curve has not been carried to energies smaller than 136 Mev, which is the energy corresponding to bursts of nominal size 2 particles or 1.26×10^5 ion-pairs (antilog 5.1), because presumably Eq. (1) is not valid for smaller bursts.

The rather involved series of operations made in arriving at the upper curve of Fig. 3 may now be checked back to the gross integral rate given in Table II of II. Integration of the upper curve yields 1.33×10^{-3} per sphere of unit area per second for the flux of electrons and photons capable of producing bursts in the ion chamber of more than the nominal size 2 particles (antilog 5.1) under a lead shield of thickness 0.67 cm. The corresponding number from Table II of II is 1620 per hour in the ion chamber (antilog 3.21). The number of bursts of more than 2 particles (nominal) generated by μ mesons in this thickness of lead may be disregarded. Dividing 1622 by 3600×324, we find a rate of 1.39×10^{-3} per sphere of unit area per second to be compared with 1.33×10^{-3}. Therefore no gross error has been made.

4. CORRECTION FOR FLUCTUATIONS

To estimate the effect of fluctuations, consider the rate $R(N)$ of cascades of N electrons emerging from a layer of fixed thickness on which electrons and photons are incident normally with an energy spectrum $S(E)$. Let $P(N,E)$ be the probability that exactly N emergent particles are produced by incident electrons or photons of energy E and let $\Pi(E)$ be the average number of emergent particles in the cascades produced by that energy. Then, if the Poisson distribution is the correct[6] one for the fluctuations,

$$P(N,E)=e^{-\Pi}\Pi^N/N!, \tag{3}$$

and the rate will be given by

$$R(N)dN=dN\int_0^\infty S(E)dE\,P(N,E)$$

$$=dN\int_0^\infty S(E)dE\frac{e^{-\Pi}\Pi^N}{N!}. \tag{4}$$

The effect of fluctuations on the value of $R(N)$ is required at that thickness of the layer which produces the maximum rate $R(N)$. Since large contributions to the integral (4) are made only by cascades initiated by particles in a small energy range, namely the energy

electrons produced by an incident particle of energy E at depth t. If we neglect the effect of fluctuations, we may write

$$R(N,t)dN=S(E)dE=S(E)\frac{\partial E}{\partial N}dN=S(E)\frac{E}{N}\frac{\partial\log E}{\partial\log N}dN,$$

and $\partial\log E/\partial\log N$ can readily be obtained from the family of curves given by Rossi.

To obtain the transition curve expected for the ion chamber as a whole it is necessary to calculate the separate curves for bursts of the same size in ion-pairs but different sizes in number of particles for a suitably large number of zones of equal area but different mean radius covering the whole area of the ion chamber and then add the resulting curves together.

[6] Both the theoretical calculations of Jánossy and Messel and the Monte Carlo calculations of Wilson support the Poisson character of the fluctuations near the shower maxima.

range corresponding to the width of the Poisson distribution (i.e., those cascades with mean numbers of particles between $\Pi-\sqrt{\Pi}$ and $\Pi+\sqrt{\Pi}$, where Π is the mean number of particles in the most effective cascades) the cascades will be treated as though they contained a constant number of particles at all thicknesses. Also the mean number of particles, for simplicity, will be taken to be exactly proportional to the incident energy and not as given by Eq. (1). Therefore we shall write

$$\Pi=KE, \quad (K=\text{const}). \tag{5}$$

The incident energy spectrum in the relevant energy range will be approximated by a power law with exponent $-\gamma$,

$$S(E)dE=CE^{-\gamma}dE, \quad (C=\text{const}). \tag{6}$$

Combining (4), (5), and (6)

$$R(N)=\frac{CK\gamma^{-1}}{N!}\int_0^\infty \Pi^{N-\gamma}e^{-\Pi}d\Pi$$

$$=\frac{CE^{-\gamma}}{K}\frac{N\gamma\Gamma(N-\gamma+1)}{N!}. \tag{7}$$

The factor $CE^{-\gamma}/K$ is the rate that would be observed if there were no fluctuations and $N\gamma\Gamma(N-\gamma+1)/N!$ is the factor by which the observed rate must be divided to correct the spectrum of Fig. 4 for the effect of fluctuations. The correction was made by trying different values of γ till an approximately self-consistent result was obtained over the whole energy range, as shown by the lower curve in Fig. 4 which is the corrected energy spectrum.

Between 136 and 1600 Mev the slope in Fig. 4 of the omnidirectional differential spectrum changes gradually from -2.20 to -2.35. Above 1600 Mev the spectrum may be represented by a power law of slope -3.00. At 1600 Mev, where the slope changes rather abruptly, the rate is 3.0×10^{-8} per sq cm per sec per Mev. For energies involving cascades of less than 2 particles at the cascade maximum the spectrum cannot be determined by this method. It is of considerable interest to integrate the spectrum in the energy range above 136 Mev and try to extend it towards lower energies by means of other information.

5. INTEGRAL ENERGY SPECTRUM

The integral spectrum is shown in Fig. 5 by the solid curve ending at 136 Mev. From the ion-chamber measurements one additional experimental point can be plotted on Fig. 5 using the rate of occurrence of electron bursts of all sizes in the unshielded ion chamber as given in Table I of I. The smallest reliably detected size of burst is 2.5×10^4 ion-pairs which corresponds to about 0.7-Mev energy release in the ion chamber (for comparison the average burst size due to a single relativistic particle is 6.3×10^4 ion-pairs corresponding

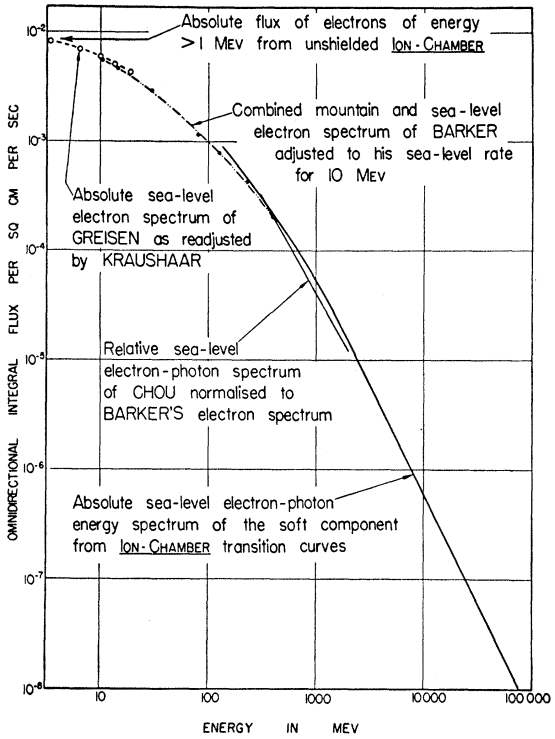

FIG. 5. The omnidirectional integral energy spectrum of the electrons and photons of the soft component near sea level compared with previous measurements made by others.

to 1.8 Mev). Therefore the rate 8.5×10^3 per hour, or 8.4×10^{-3} per sphere of unit area per sec, can be taken as a measure of the flux of electrons of energy greater than 0.7 Mev. As an argument that this rate may be fairly accurate it should be noted that the omnidirectional flux of μ mesons in the ion chamber, yielding bursts larger than this size (2.5×10^4 ion-pairs), is given in the same table as 1.95×10^4 per hour which happens to agree exactly with the accepted flux of μ mesons near sea level, 1.68×10^{-2} per sphere of unit area per sec, for a sphere of 324 sq cm.

Before the total flux of electrons is plotted in Fig. 5 the rate should perhaps be increased to make it consistent with the remainder of the graph. This is because the graph includes the flux of photons as well as electrons and it is generally believed that these are about equal in number at sea level at energies around 100 Mev. For the present, however, the rate for the electrons only has been used for the additional experimental point in Fig. 5.

6. COMPARISON WITH OTHER MEASUREMENTS

The results of other experiments giving the energy spectrum of the soft component near sea level are shown in Fig. 5. Greisen[7] measured the integral energy spectrum of electrons over the range from 3.4 to 18.9 Mev,

[7] K. Greisen, Phys. Rev. **63**, 323 (1943).

using an essentially omnidirectional Geiger counter arrangement with carbon absorbers. His absolute intensity at 10 Mev was readjusted by Kraushaar[8] from 0.0041 to 0.0060 per sq cm per sec and in Fig. 5 Greisen's experimental points have been readjusted by this factor. Barker[9] more recently has given the integral spectrum of electrons up to 395 Mev obtained by means of a very narrow-angle counter telescope used in conjunction with a cloud chamber containing absorbing plates. The spectrum given by Barker is a relative one obtained by adding together sea level and mountain data but he gives a figure for the absolute rate of all electrons of energy greater than 10 Mev near sea level (0.0056 ± 0.0005 cm^{-2} sec^{-1}) and his relative curve has been adjusted to this rate in Fig. 3. The experimental points were plotted from figures kindly provided by Dr. Barker and the curve drawn through them differs slightly from the one given in his paper. Chou[10] used two large plastic scintillators sandwiching a lead plate and he measured only relative rates (for the electrons and photons separately) between 300 and 2000 Mev. In his case therefore the curve reproduced in Fig. 5 shows only the *shape* of the combined electron-photon spectrum at sea level.

The results of other measurements, mostly relative and mostly at mountain elevations, have been summarized by Puppi[11] who makes the comment, writing in 1954 before Barker's paper appeared, that, "as to the shape of the spectrum of this component and its variation with depth · · · the information which we possess today is not very great."

7. RANGE AND ACCURACY OF THE ENERGY SPECTRUM

The range of energy covered in the present work greatly exceeds that of previous investigations. The range is 200 times that measured by Barker and 30 times that investigated by Chou.

Three separate considerations are involved in assessing the probable accuracy. The first concerns the measurements and their analysis as far as the curve reproduced in Fig. 3; the second is the conversion from ion-pairs to effective numbers of particles; the third is the use of cascade theory to convert from numbers of particles to energies.

The basic observation consists of counting the number of bursts larger than a given size that occur in a suitable time interval. Hence the accuracy of the determination of pulse size is the principal factor that must be discussed with regard to Fig. 3 and this involves review of the procedure used for routine calibration of the apparatus.

Calibration pulses, continuously variable in size, were injected into the ion-chamber collecting electrode through a fixed air-dielectric condenser using a step-voltage provided by a precision helical potentiometer calibrated against a standard cell. Charge injected into the system in this manner is exactly equivalent to charge injected by ionization in the ion chamber. The output was measured in four different ranges of size (by, respectively, a scaler, a 10-channel pulse-height analyzer, and two recording pens) so as to cover a range of pulse size of more than three decades between about 2.5×10^4 ion-pairs and 10^8 ion-pairs. The accuracy of measurement of the output pulses within each range of size varied but it can be taken that the larger pulses in each range were determined with a relative accuracy of $\pm1\%$.

The absolute accuracy of pulse size in ion-pairs depends upon the figure used for the capacity of the injection condenser. Limits of $\pm2\%$ were quoted for this in I. The sizes given in I, II, and in this paper, in ion-pairs, are absolute within this accuracy except for the correction ($+11\%$ on the average, see I) for the fact that only the negative-ion contribution to pulse size is measured: however, the absolute size of the bursts in ion-pairs has not been required for the establishment of the energy spectrum as deduced in the present paper.

The above estimate of the relative accuracy of the pulse-size calibration is upheld by the self-consistency of the measurements. During more recent experiments of a few weeks duration at 10 700 feet altitude, in a period of quiet sun, the measured rates were consistent after barometer correction to $\pm2\%$, which implies pulse-height consistency to $\pm1\%$. The measurements contributing to Fig. 3 extended over about three years and appeared to be consistent in rate at least within $\pm10\%$ whenever the bursts recorded were not so few that the statistical accuracy was poor.

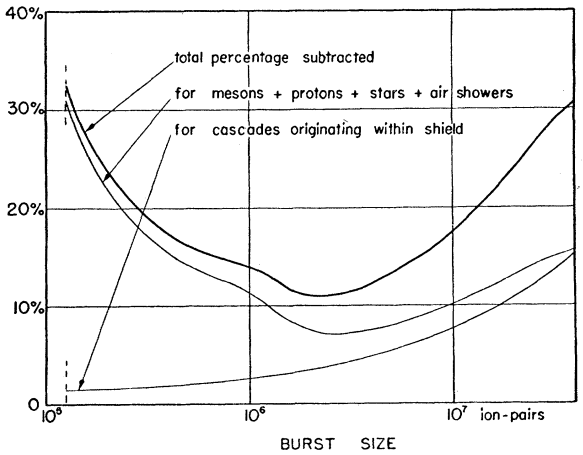

FIG. 6. The approximate percentages of the observed gross rates at the maxima of the transition curves which were subtracted to correct for bursts due to μ mesons, protons, stars, and extensive showers and for bursts due to cascades engendered in the lead shield.

[8] W. L. Kraushaar, Phys. Rev. **76**, 1045 (1949).
[9] P. R. Barker, Phys. Rev. **100**, 860 (1955).
[10] C. N. Chou, Phys. Rev. **90**, 473 (1953).
[11] G. Puppi, *Progress in Cosmic-Ray Physics* (North Holland Publishing Company, Amsterdam, 1956), p. 371.

Next, we have to consider that sundry subtractions were made before the rates plotted in Fig. 3 were found. The percentages that were subtracted are indicated in Fig. 6. The rates all come from the *maxima* of the transition curves so that the situation is favorable as regards the proportion subtracted. From just above pulse size 10^5 ion-pairs and for all larger sizes the proportion subtracted representing the sum of the μ-meson, proton, star, and extensive shower components is always less than 30%, and in general less than 15%, of the measured rate. The proportion subtracted on account of the cascades that are engendered within the lead varies from only a few percent for the small bursts to about 15% for the largest bursts. Thus, in general these subtractions have little effect on the accuracy. Therefore, allowing for some improvement from the graphical smoothing, the relative accuracy of the rates of Fig. 3, between pulse sizes 10^5 ion-pairs and 10^7 ion-pairs, can be given as $\pm 5\%$. Beyond 10^7 ion-pairs the statistical inaccuracy of the counting supervenes. The radius of the experimental points shown on Fig. 3 represents 7% in the rate and 3.5% in the size.

Next, the conversion from ion-pairs to the average number of electrons in the cascades must be considered. There are two ways of finding the conversion factor. One, which we have not used except as a check, depends upon the absolute electrical calibration of the ion chamber and is potentially the more accurate. It was used for the comparison of calculated and measured μ-meson bursts shown in Fig. 9 of I. One uncertainty of this method is the figure to be used for the average number of electron volts per ion-pair for argon at 50 atmos pressure, since there may be some loss of ions by columnar recombination.

The conversion factor that was used, 6.3×10^4 ion-pairs per relativistic electron, was determined from the shape of the μ-meson pulse-height distribution. The figure was checked (see Fig. 7 of II) by a comparison with the Carnegie Meter data for the rate of large bursts under 12 cm of lead. The agreement was within the statistical accuracy of our observations for the rather infrequent large bursts involved. The limits of error by this method should be set at $\pm 10\%$ in the conversion factor or about $\pm 20\%$ in the rates.

At present the final conversion from particle number to energy is the most uncertain step but it can be improved when dependable theoretical data becomes available. Consider, for example, the factor 2 that was introduced in Eq. (2). The energy value assigned to any of the measured rates in the spectrum is directly proportional to this factor so the rate assigned at a particular value of the energy will be proportional to this factor to the power γ, where $-\gamma$ is the exponent of the spectrum. Thus, in a region where the integral spectrum varies as E^{-2} the rate would be increased 21% by a 10% increase of the factor 2. The present writer is not prepared to assign firm limits of error to the factor 2 that has been used. It might nevertheless be safe to say that the rate given in the integral spectrum of Fig. 5 is certainly within a factor 2 of the correct absolute value and that, allowing for the uncertainty of the correction for fluctuations, the relative rate, or the shape of the curve, is correct to within $\pm 20\%$.

The question of the possible influence of secondary photons and cascade electrons generated in the atmosphere and accompanying the highest energy electrons closely enough to intersect the ion chamber is left open for the present. There is no doubt that this must occur but possibly the effect upon the spectrum as obtained from the rates at the maxima of the transition curves is small.

8. ACKNOWLEDGMENTS

The writer is grateful to Dr. K. Greisen for reading a draft of this paper. Invaluable advice with regard to the calculations was generously given by Dr. T. D. Newton of the Theoretical Branch of this laboratory. The accurate measurements on which this work is based are primarily due to J. F. Steljes.